Validation of Wind Loads on a Slender Vessel using CFD

Jonathan W. Vogt[*], Marco Bovio[§], and Benoit Mallol[‡]
[*]Damen Shipyards, Singapore, [§]Damen Shipyards, Gorinchem/Netherlands, [‡]NUMECA International, Brussels/Belgium
jonathan.vogt@damen.com

1 Introduction

The IMO regulation 749.18, 'Severe wind and rolling criterion (weather criterion)', ensures a vessel has sufficient transversal stability to resist over-rolling in severe side winds. For some long, slender vessels, however, it can be difficult to comply with the empirical requirements of this regulation. To account for such difficulties, the regulation allows for the demonstration of compliance by means of model scale experimental measurements – from both a towing tank and wind tunnel campaign. In so doing, the hydrodynamic and aerodynamic lever arms, under side wind conditions, can be determined for various heeling angles and assessed as to whether the vessel is compliant and able to operate unrestricted.

Due to the necessarily conservative nature of the regulation (enabling it to be broadly applicable to a multitude of vessels), slender vessels like the DAMEN Fast Crew Support (FCS) 3307 have difficulties in satisfying the empirical requirements of the regulation, thus necessitating expensive experimentation in order to demonstrate the vessel's compliance with the regulation. In order to reduce the cost of proving compliance, DAMEN is developing, in partnership with its Computational Fluid Dynamics (CFD) code supplier NUMECA International, a CFD methodology that can be used in lieu of experimentation. This validation project has been undertaken with the intention of being able to demonstrate compliance to the satisfaction of classification societies.

The CFD methodology described here is focused on the prediction of the aerodynamic forces only. As the motivation for using the CFD approach is primarily cost and time related, it is imperative that the methodology be both sufficiently accurate but also with as low as possible computational cost and total turnaround time. The methodology reflects these aims.

The establishment of robust procedures in the literature for the accurate numerical modelling of wind loads over maritime vessels, is lacking. A small number of researchers have simulated flow over wind-exposed hulls and superstructures of various forms, with differing approaches and levels of fidelity. Validation for these cases (comparing either velocity probe or force data) was generally quite good in qualitative terms, while sometimes insufficient in quantitative terms (Polsky, 2002; Wnęk and Guedes Soares, 2015; He, *et al*. 2016).

A thoroughly and successfully validated investigation was undertaken by Forrest and Owen (2010), who performed full-scale Detached-Eddy Simulations (DES) of the flow field over a navy frigate in order to predict the flow field encountered at the helicopter landing pad on the vessel's rear deck. The model was validated against model-scale experimental hot-probe velocity data. The scale difference between the simulation and experiment was disregarded as the scale effect was demonstrated to be minor. Using an unstructured mesh of 7.4×10^6 cells, a relatively large normalised timestep $\Delta t^* = 0.0188$ (normalised by wind speed and vessel beam) and the k-ω SST turbulence model, good qualitative agreement was seen for the time-averaged flow field over the landing pad and in the Power Spectral Density (PSD) comparisons of velocity, at various points on the ship.

The present paper reports the results of a CFD validation campaign where a wind tunnel test of the DAMEN FCS3307 vessel was numerically replicated. The vessel and wind tunnel CFD domain is shown in Fig. 1.

2 Experiment

The experiment was undertaken at the University of Southampton wind tunnel using a 1:18 scale model of the 33m long FCS3307 vessel. The institute provided the 3D geometry of the testing facility, in order to allow a realistic reproduction of the environmental test conditions in the CFD model. The testing was conducted at various heading and heeling angles and also with and without containers on the rear deck of the vessel, to take account of the different operating configurations of this unit. The model was kept

at a constant longitudinal (zero) trim while maintaining the same displacement at different heeling angles. The model and sting were mounted in a small pool of water around the model (with the waterline flush with the floor of the tunnel), to avoid air recirculation under the model. The tests were all performed at a freestream velocity of approximately 7m/s, maintaining the flow above the critical Reynolds number (Re), (about 2.7×10^5, based on the vessel beam). Additionally, turbulence was introduced to the tunnel through screens which further raised the effective Reynolds number. The boundary layer profile at the test section was measured (without the model installed) and this was used to calibrate the CFD model. The results, against which the CFD model was compared, were corrected for tare drag (less than 2% of the measurements, in all cases) but were not corrected for blockage effects, allowing for a like-for-like comparison with the CFD model.

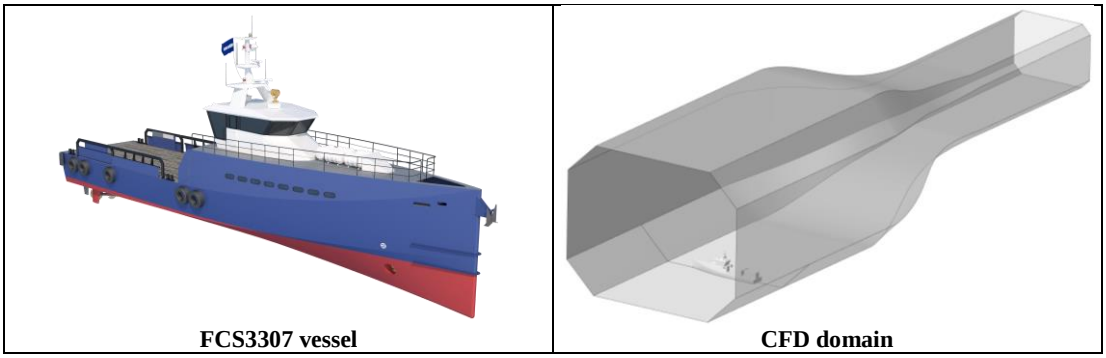

Fig. 1: Vessel and CFD domain.

3 Conceptual Model and Numerical Mesh

The computational domain reproduced the test-section and downstream contraction of the University of Southampton wind tunnel. This arrangement allowed for the faithful reproduction of flow field and blockage conditions apparent in the experiment. Turbulence screens upstream of the test section increased the turbulence and also straightened the flow after a 90° corner in the tunnel circuit.

Measurements taken in the empty tunnel showed a semi-developed and highly turbulent boundary layer. It has been shown in the literature that correctly reproducing the atmospheric boundary layer profile is essential for modelling accuracy (Polsky, 2002; Forrest and Owen, 2010). To correctly reproduce the boundary layer velocity profile, the numerical model required a distance of approximately 3m to the centre of the test section, employing a Turbulence Intensity (TI) of 10%. This value was determined through trial-and-error as the experimental TI was not recorded. To correctly characterise the profile, it was necessary to fully resolve the boundary layer on the floor of the tunnel, from the inlet to the installed model. A comparison of the measured and simulated boundary layer velocity profiles (at the test section, without the model) is shown in Fig. 2.

With a view to facilitating the quickest and simplest model preparation, the water pool in the wind tunnel was not included in the CFD model. Rather, the model was simply truncated at the solid tunnel floor with the submerged portion of the model disregarded. The resulting solid surfaces of the model do not form a sealed volume (with an opening at the tunnel floor), leading to a significant imbalance in the resultant vertical force acting the on model. This was accounted for in the CFD model by applying a vertical correction force acting at the centroid of the model-tunnel floor cross-section. The correcting force was defined as the ambient pressure in the domain, multiplied by the cross-sectional area. This vertical force vector also provided corrections for pitch moment and heeling moment.

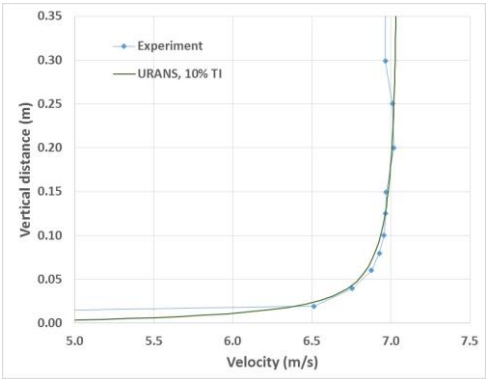

Fig. 2: Boundary layer velocity profile.

The numerical mesh was generated with the mesher Hexpress Hybrid, by Numeca, which is a general purpose script-based automatic mesher that generates hex-dominant unstructured meshes about arbitrary and complex geometry. An initial mesh sensitivity study using a URANS solver,

testing meshes between 8×10^6 and 182×10^6 cells, informed an initial mesh density that ultimately produced meshes between 10-13$\times10^6$ cells, depending on the model arrangement.

The mesh concentrated spatial refinement on the model and wind tunnel surfaces. Two refinement boxes were used around the vessel and in its wake, to capture the flow details with more fidelity. All sharp edges on the model had increased refinement. The wind tunnel floor had a fully resolved boundary layer mesh from the inlet to the model, with a y^+ of approximately 0.4. The remainder of the wind tunnel walls used wall functions and had y^+ values of approximately 28. Due to the bluff nature of the ship model and the expectation of separation at sharp corners, the model boundary layer mesh also used wall functions, with a thickness of only three cells and y^+ less than 30. The viscous component of the forces acting on the model were expected to be extremely small, and with no smooth surface separation or opportunity for boundary layer development, there was no need for a detailed boundary layer mesh. The mesh is shown in Fig. 3.

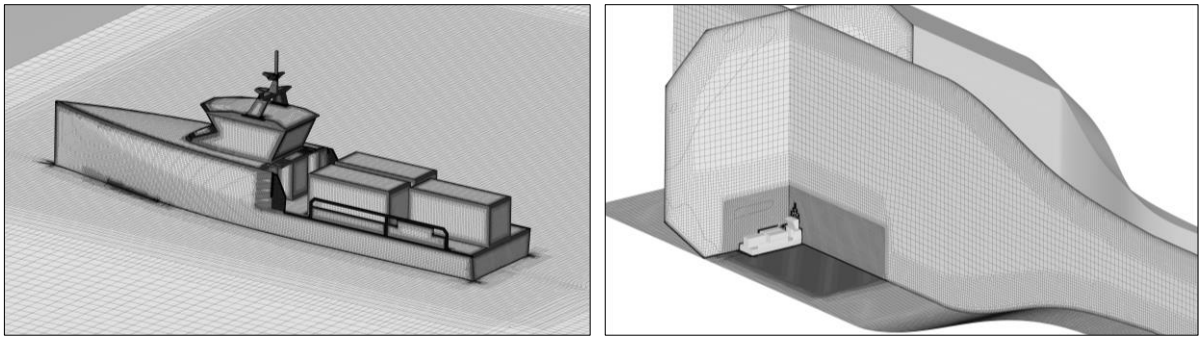

Fig. 3: Numerical mesh, heading = 90°, heel = 0°.

4 Numerical Settings

The solver FINE/Marine v6.1, by Numeca, was used for all simulations. It utilises the finite-volume method for the solution of the incompressible Navier-Stokes equations. It is an unstructured, face-based, segregated solver and its fully unsteady solver utilising an implicit 2nd-order accurate temporal discretisation scheme.

The mesh was prepared with the intention to compare the effectiveness of both the Unsteady Reynolds-Averaged Navier-Stokes (URANS) solver approach and the DES approach. DES has the advantage of being able to explicitly resolve the large scales of turbulence, which is particularly advantageous for large scale separation off bluff bodies. The DES model switches between an explicit resolution of the larger turbulent scales or a turbulence model calculation, based on the local mesh cell size. If the cell is not small enough to capture the larger scales, the DES model will be inactive and effectively behaves as a URANS solver.

The for URANS solver, the convective terms were discretised using the AVLSMART scheme (Pržulj and Basara, 2001), which is based on the 3rd-order QUICK scheme. For the DES solver, the convective terms were discretised using a blended scheme between 1st-order upwinding and central-differencing, with a 5% weighting to upwinding. The turbulence model used was the Explicit Algebraic Stress Model (EASM), which is based on the k-ω SST model but better accounts for the rotational component of turbulent flows.

A constant velocity V = 6.98m/s was applied at the inlet. With development of the boundary layer, the freestream velocity reaches 7m/s at the ship model. The turbulent quantities at the inlet were set to $k = 2.1565\times10^{-7}$ m^2/s^2 and ω = 14.0 /s (= V_{ref}/L_{ref}), which corresponds to a TI = 10%. The tunnel outlet was set to a constant pressure outlet. The tunnel floor from the inlet to the model was set to a no-slip wall with fully resolved boundary layer. The ship model and remaining tunnel walls were set to no-slip walls, employing a wall function. The domain was initialised with zero velocity components and the same turbulence quantities as at the inlet.

Timestep sensitivity studies were undertaken for both URANS and DES approaches. The present mesh was temporally independent with a timestep of Δt_{URANS} = 0.1s for URANS. For the DES solver, no change in the temporally-averaged forces and moments were observed with a timestep smaller than

Δt_{DES} = 0.01s. This was considered quasi-temporal independence for the DES solver. When normalised in the same way as Forrest and Owen (2010), $\Delta t_{DES}^* = 3.67\times10^{-3}$, which is only one-fifth of the normalised timestep employed in that study. The URANS cases solved 10 iterations per timestep, while the DES cases solved 15 iterations per timestep. DES was tested with 20 iterations per timestep, but this was shown to have negligible effect on the averaged forces.

In order to approach the solution as quickly as possible and reduce the overall solution time, an initial steady-state RANS simulation was conducted for just 100 iterations. This short simulation was sufficient to develop the flow field to a point such that it was a good starting point for both the DES and URANS models. This saved significant flow development time for both solution strategies.

The URANS cases, initialised from the steady state run, computed between 700 and 1500 timesteps, depending on the model arrangement. The simulation was run until the forces, moments and residuals had settled to a constant value. The DES cases were first computed for 150 timesteps to overcome the transient phase and achieve quasi-steadiness. A data averaging simulation was then initialised from this run and computed for about 1000 more timesteps (180 flow times across the model beam).

The simulations conducted are shown in Table 1, indicating the heading and heel angles and whether or not the containers on the deck were included. A heading angle of zero represents a bow into the wind condition, 90° is wind onto the portside. A positive heel angle represents the ship leaning away from the wind. The model including the containers increased the frontal area of the model (at heading of 90°) by 19%. A full sweep of heading angles were simulated with and without containers with the URANS solver and, at full side wind (heading of 90°), three different heeling angles were also simulated with the URANS solver. The DES solver was used for selected container cases at zero heel angle.

5 Results and Discussion

Table 1: Simulated cases.

	Heel (°)				
	-10	**0**		**20**	**40**
Heading (°)	**w. cont.**	**w. cont.**	**w/o. cont.**	**w. cont.**	**w. cont.**
30		URANS, DES	URANS		
60		URANS	URANS		
90	URANS	URANS, DES	URANS	URANS	URANS
120		URANS, DES	URANS		
150		URANS, DES	URANS		

The results for the zero-heel cases, alongside the experimental results, are shown in Fig. 4. They are presented in terms of the forward (to bow), side (to starboard) and vertical (upward) forces, and the pitching, heeling and yaw moments. Very good qualitative agreement is found, both with and without containers. The agreement at the 90° heading case (side-on to the wind) is the most favourable – the side force is predicted within 12% without containers and within 4% with containers. For all headings, the solved forces generally achieved a lower percentage error than did the moment results, but the discrepancy was very similar in absolute terms. The CFD model tended to be further from the experimental results at heading angles increasingly distant from 90°, in both directions. This may be due to the increasing non-alignment of the freestream mesh cells with the ship model and the resulting complex tetrahedral mesh that is imposed near the ship surface.

The DES results in Fig. 4 indicate that, in general, the DES solver is slightly superior to the URANS solver, in terms of the calculation of forces and moments. The side force prediction, in particular, is significantly improved with the DES solver. It produced a less accurate result for the vertical force and relatively unchanged or slightly better for the forward force and the three moments.

The results for the heeled case are shown in Fig 5. The qualitative agreement is again very good, however, the correlation generally deteriorates at heel angles increasingly distant from zero and, again, in both directions. With the current, limited mesh refinement, discretisation errors may be contributing to the errors seen on the more extreme cases.

The URANS solver was not able to capture the inherent highly turbulent nature of the flow field, which is demonstrated quantitatively in Fig. 6 and qualitatively in Fig. 7. Both figure compare a URANS result against an instantaneous DES result. The URANS solution shows no evidence of time-dependant turbulent eddies, whereas the DES solution shows significant turbulent behaviour and a very high level of mixing. Although there is some local variation in the forces acting on the vessel (see Fig. 6), the position of the centre of pressure varied very little, not exceeding $0.01L_{pp}$.

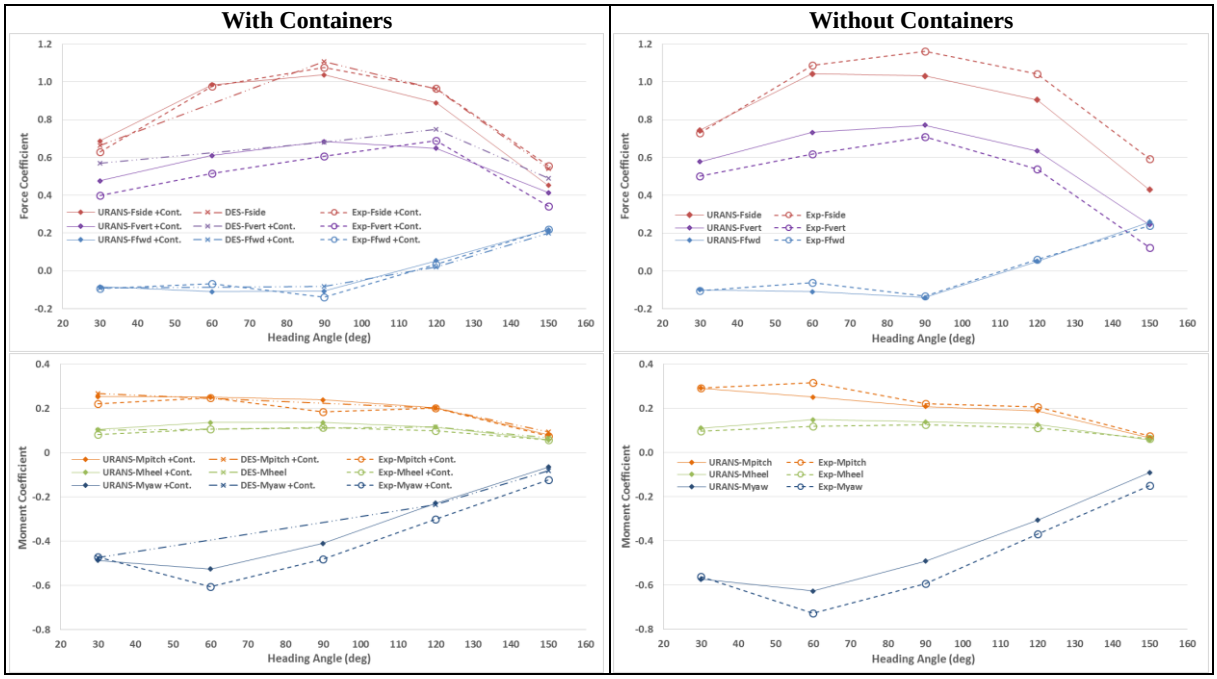

Fig. 4: Force and moment results for zero-heel cases, with and without containers.

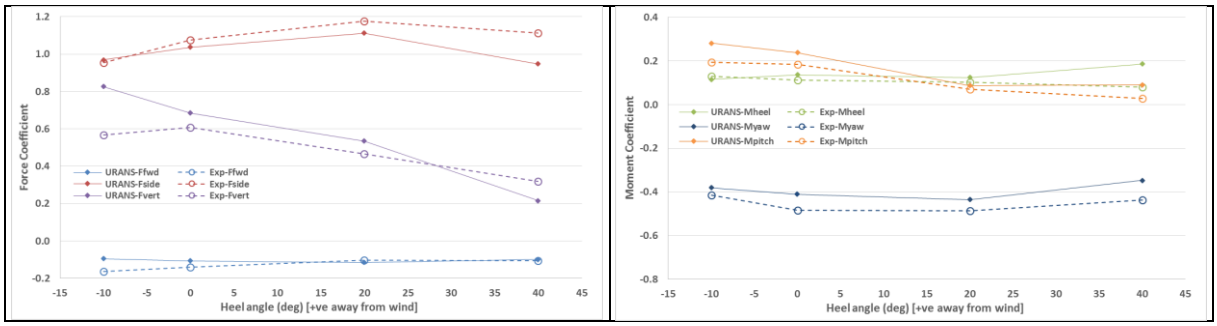

Fig. 5: Force and moment results for heeled cases, heading angle = 90°, with containers.

The DES solution is clearly capable of capturing more of the physical character of the flow and so could be beneficial in the determination of frequency domain information about the flow's interaction with the vessel, or perhaps useful statistical information about the loads and moments on the vessel. However, for obtaining the averaged force and moment data only, the URANS solver would appear to be an adequate approach, and slightly more cost effective than DES.

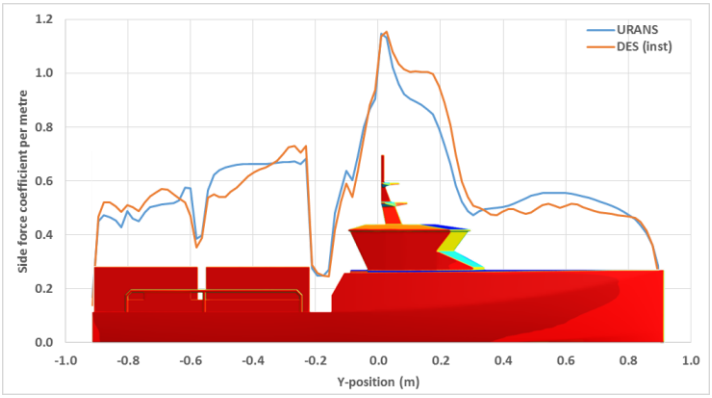

Fig. 6: Side force distribution; heading 90°, heel 0°.

6 Conclusion

A CFD validation study was undertaken to develop an affordable numerical modelling methodology that may be used for the determination of wind loads on model ships, without the need for expensive wind tunnel experiments. Both URANS and DES approaches were investigated. The CFD model reproduced the validation wind tunnel experiment and tunnel apparatus and achieved good correlation for forces and moments at various heading and heeling angles. The DES methodology was favourable in terms of its ability to capture the flow features. It also achieved slightly better correlation with the experimental data. The URANS solution, though unable to capture the temporal character of the flow, was able to predict the forces and moments with good accuracy and was also slightly cheaper to run than the DES solver. Given the highly turbulent nature of this bluff-body separation problem, prediction

of full-scale loads should be quite reliable. Future work will seek to adapt this methodology to full-scale prediction, with only minor changes anticipated.

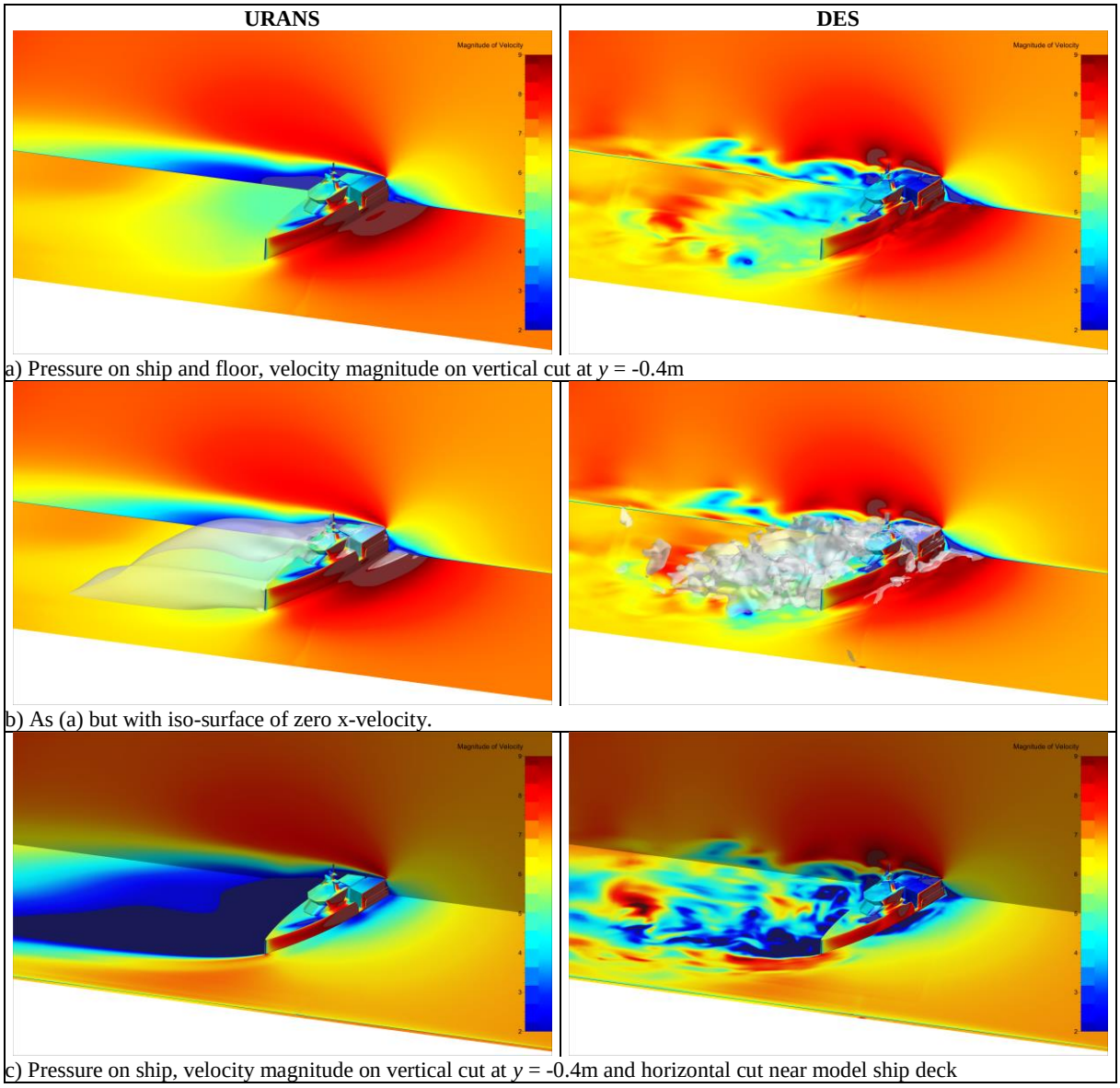

Fig. 7: Qualitative comparison of flow field; heading 120°, heel 0°.

References

J.S. Forest and I. Owen (2010). An investigation of ship airwakes using Detached-Eddy Simulation, *Computers and Fluids*, **39**, 656-673.

N.V. He, K. Mizutani and Y. Ikeda (2016). Reducing air resistance acting on a ship by using interaction effects between the hull and accommodation, *Ocean Engineering*, **111**, 414-423.

S.A. Polsky (2002). A computational study of unsteady ship airwake. Proceedings of 40th AIAA Aerospace Sciences Meeting & Exhibit, Reno, USA.

V. Pržulj and B. Basara (2001). Bounded Convection Schemes for Unstructured Grids. Proceedings of AIAA Computational Fluid Dynamics Conference, Anaheim, USA.

A. D. Wnęk and C. Guedes Soares (2015). CFD assessment of the wind loads on an LNG carrier and floating platform models, *Ocean Engineering*, **97**, 30-36.